
CDF TRANSFORM-SHIFT: AN EFFECTIVE WAY TO DEAL WITH INHOMOGENEOUS DENSITY DATASETS

A PREPRINT

Ye Zhu✉

School of Information Technology
Deakin University
Victoria, Australia 3125
ye.zhu@ieee.org

Kai Ming Ting

School of Information Technology
Federation University
Victoria, Australia 3842
kaiming.ting@federation.edu.au

Mark J. Carman

Faculty of Information Technology
Monash University
Victoria, Australia 3800
mark.carman@monash.edu

Maia Angelova

School of Information Technology
Deakin University
Victoria, Australia 3125
maia.a@deakin.edu.au

December 15, 2024

ABSTRACT

Many distance-based algorithms exhibit bias towards dense clusters in inhomogeneous datasets (i.e., those which contain clusters in both dense and sparse regions of the space). For example, density-based clustering algorithms tend to join neighbouring dense clusters together into a single group in the presence of a sparse cluster; while distance-based anomaly detectors exhibit difficulty in detecting local anomalies which are close to a dense cluster in datasets also containing sparse clusters. In this paper, we propose the CDF Transform-Shift (CDF-TS) algorithm which is based on a multi-dimensional Cumulative Distribution Function (CDF) transformation. It effectively converts a dataset with clusters of inhomogeneous density to one with clusters of homogeneous density, i.e., the data distribution is converted to one in which all locally low/high-density locations become globally low/high-density locations. Thus, after performing the proposed Transform-Shift, a single global density threshold can be used to separate the data into clusters and their surrounding noise points. Our empirical evaluations show that CDF-TS overcomes the shortcomings of existing density-based clustering and distance-based anomaly detection algorithms and significantly improves their performance.

Keywords Density-ratio · Density-based Clustering · kNN anomaly detection · inhomogeneous densities · Scaling · Shift

1 Introduction

Many distance-based algorithms have a bias towards dense clusters^{2,5,13,36,26}. For example, (i) DBSCAN¹² is biased towards grouping neighbouring dense clusters into a single cluster, in the presence of a sparse cluster³⁶. (ii) The k NN anomaly detector^{4,27} employs the k NN density estimator^{16,23} to estimate the density of every point in a dataset, and then sorts all the points based on their estimated density in descending order. Low-density points are regarded as more likely to be anomalous than high-density points. Since the ranking is based on global densities, this bias results in the misclassification of so-called “local anomalies” (points considered anomalous with respect to their neighborhood) in high density regions as normal points^{7,8,9}.

A number of techniques have been proposed to “correct” this bias, notably, the density-ratio approach of ReCon³⁶, ReScale³⁶ and DScale³⁷ (for density-based clustering such as DBSCAN¹⁴ and DP²⁹), and the reachability-distance approach of LOF⁷ (for the k NN anomaly detector²⁷).

The density-ratio approach^{36,37} aims to transform the data in such a way that the estimated density of each transformed point approximates the density-ratio of that point in the original space, and as a result all locally low-density points are easily separated from all locally high-density points using a single global threshold.

While the current density-ratio methods have been shown to improve the clustering performance of density-based clustering, we identify their shortcomings and propose a new algorithm to better achieving the aim of the density-ratio approach. Furthermore, we extend its application to distance-based anomaly detection.

We propose to perform a multi-dimensional Cumulative Distribution Function (CDF) based transformation on the given dataset as a preprocessing step, which learns a mapping f^1 such that the resulting Euclidean distance between pairs of points $d(\mathbf{x}, \mathbf{y}) = \|f(\mathbf{x}) - f(\mathbf{y})\|_2$ is “locally consistent” with the Euclidean distance between points in the original space (i.e., all local inter-point distances are proportional to their original values), while the final transformed dataset has a uniform distribution, as estimated by density estimator pdf using a certain bandwidth. This effectively achieves the desired aim of CDF transform, i.e., density equalisation w.r.t. a density estimator with a certain bandwidth, without impairing the cluster structure in the original dataset.

This paper makes the following contributions:

- (1) It generalises a current CDF scaling method DScale³⁷ so that it can be applied to density estimators using uniform kernels with either fixed or variable bandwidths.
- (2) It proposes a new Transform-Shift method called CDF-TS (CDF Transform-Shift) that changes the volumes of each point’s neighbourhood simultaneously in the full multi-dimensional space. Existing CDF transform methods are either individual attribute based (e.g., ReScale³⁶) or individual point based (e.g., DScale³⁷). As far as we know, this is the first attempt to perform a multi-dimensional CDF transform to achieve the desired effect of homogenising (making uniform) the distribution of an entire dataset w.r.t a density estimator.
- (3) It applies the new Transform-Shift method to density-based clustering and distance-based anomaly detection to demonstrate its impact in overcoming the weaknesses of three existing algorithms.

The proposed approach CDF-TS differs from existing approaches in terms of:

- (i) **Methodology:** While ReScale³⁶, DScale³⁷ and the proposed CDF-TS follow the same principled approach and have the same aim, the proposed CDF Transform-Shift method is a multi-dimensional technique which incorporates both transformation and point-shift, which greatly expand the approach’s applicability. In contrast, ReScale is a one-dimensional transformation and point-shift technique; and DScale incorporates transformation without point-shift. The ‘complete’ CDF-TS method leads to a better result in both clustering and anomaly detection, which we will show in Section 6.
- (ii) **Metric compliance:** CDF-TS and ReScale create a similarity matrix which is a metric; whereas the one produced by DScale³⁷ is not a metric, i.e., it does not satisfy the symmetry or triangle inequalities.
- (iii) **Ease of use:** Like Rescale, CDF-TS transforms the data as a preprocessing step. The targeted (clustering or anomaly detection) algorithm can then be applied unaltered to the transformed data. In contrast, DScale requires an algorithmic modification in order to use it.

To demonstrate the effects of different dissimilarity measures on image segmentation, we took the image shown in Figure 1a, and applied different rescaling methods (no rescaling, ReScale, DScale and CDF-TS) and clustering the 3-dimensional pixel values of the image in LAB space³². Tables 1 show the results of applying the clustering algorithm DP²⁹ to produce three clusters. The scatter plots in LAB space in Figure 1 show that the three clusters become more uniform distributed with similar density and the gaps between their boundaries are much larger for CDF-TS than the other three scaling methods. As a result, DP with CDF-TS yields the best clustering result, shown in Table 1.

The rest of the paper is organised as follows. We describe issues of inhomogeneous density in density-based clustering and distance-based anomaly detection in Section 2. Section 3 provides the density-ratio estimation as a principle to address the issues of inhomogeneous density. Section 4 presents the two existing CDF scaling approaches based on density-ratio. Section 5 proposes the local-density transform-shift as a multi-dimensional CDF scaling method. Section 6 empirically evaluates the performance of existing density-based clustering and distance-based anomaly detection algorithms on the transformed-and-shifted datasets. Discussion and the conclusions are provided in the last two sections.

¹The mapping $f(x; D, pdf)$ depends on all points in the given dataset D , where each point $y \in D$ asserts a (local and point-based) scaling factor $r(y; pdf)$ to x .

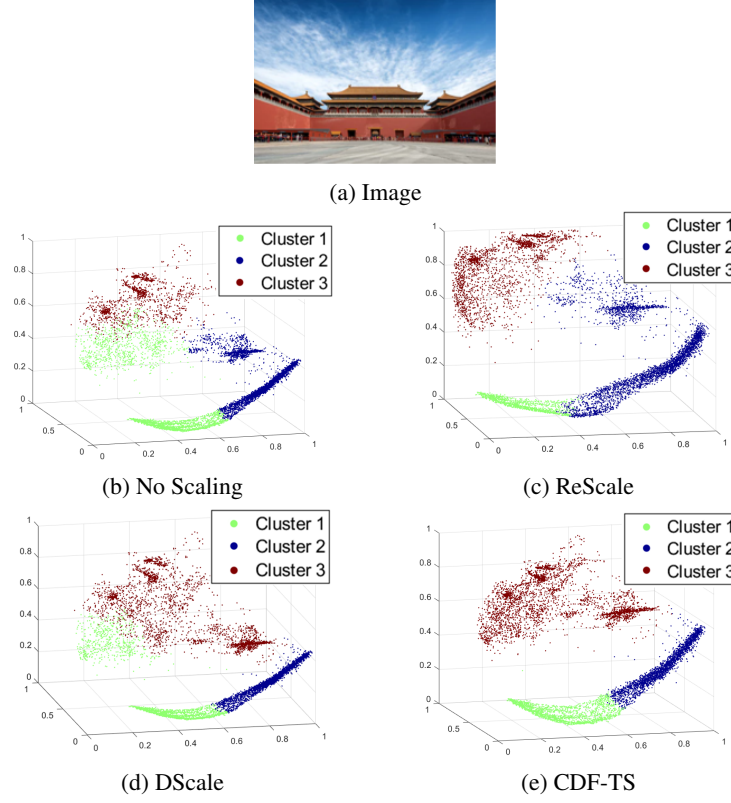


Figure 1: Clustering results by DP in LAB space of the image shown in (a). The colours in the scatter plots indicate the three clusters identified by DP using each of the four methods. The scatter plots of DScale and No Scaling are based on the original LAB attributes; and the other two are based on the transformed attributes.

Table 1: DP's image segmentation on the image shown in Figure 1a.

	Cluster 1	Cluster 2	Cluster 3
No Scaling			
ReScale			
DScale			
CDF-TS			

2 Issues of inhomogeneous density

2.1 Density-based clustering

Let $D = \{x_1, x_2, \dots, x_n\}$, $x_i \in \mathbb{R}^d$, $x_i \sim F$ denote a dataset of n points, each sampled independently from a distribution F . Let $\widehat{pdf}(x)$ denote the density estimate of point x which approximates the true density $pdf(x)$. In addition, let $\mathcal{N}(x; \epsilon)$ be the ϵ -neighbourhood of x , $\mathcal{N}(x; \epsilon) = \{y \in D \mid s(x, y) \leq \epsilon\}$, where $s(\cdot, \cdot)$ is the distance function ($s : \mathbb{R}^d \times \mathbb{R}^d \rightarrow \mathbb{R}$).

In general, the density of a point $pdf(x)$ can be estimated via a small ϵ -neighbourhood (as used by the classic density-based clustering algorithm DBSCAN¹⁴) defined as follows:

$$\widehat{pdf}_\epsilon(x) = \frac{1}{nV_\epsilon} |\mathcal{N}(x; \epsilon)| = \frac{|\{y \in D \mid s(x, y) \leq \epsilon\}|}{nV_\epsilon} \quad (1)$$

where $V_\epsilon \propto \epsilon^d$ is the volume of a d -dimensional ball of radius ϵ .

A set of clusters $\{C_1, \dots, C_\varsigma\}$ is defined as non-empty and non-intersecting subsets: $C_i \subset D$, $C_i \neq \emptyset$, $\forall i \neq j$ $C_i \cap C_j = \emptyset$. Let $c_i = \arg \max_{x \in C_i} \widehat{pdf}(x)$ denote the mode (point of the highest estimated density) for cluster C_i ; and $p_i = \widehat{pdf}(c_i)$ denote the corresponding peak density value.

DBSCAN uses a global density threshold to identify core points (which have densities higher than the threshold); and then it links neighbouring core points together to form clusters¹⁴. It is defined as follows.

Definition 1. A core point is a point with an estimated density above or equal to a user-specified threshold τ , i.e., $(\widehat{pdf}_\epsilon(x) \geq \tau) \leftrightarrow \text{Core}(x) = 1$, where Core denotes a set indicator function.

Definition 2. Using a density estimator with density threshold τ , a point x_1 is density connected with another point x_p in a sequence of p unique points from D , i.e., $\{x_1, x_2, x_3, \dots, x_p\}$: $CON_\epsilon^\tau(x_1, x_p)$ is defined as:

$$CON_\epsilon^\tau(x_1, x_p) \leftrightarrow \begin{cases} (i) \text{ if } p = 2 : \\ \quad (x_1 \in \mathcal{N}_\epsilon(x_p)) \wedge (\text{Core}(x_1) \vee \text{Core}(x_p)); \\ (ii) \text{ if } p > 2 : \\ \quad \exists_{(x_1, x_2, \dots, x_p)} ((\forall_{i \in \{2, \dots, p\}} x_{i-1} \in \mathcal{N}_\epsilon(x_i)) \wedge (\forall_{i \in \{2, \dots, p-1\}} \text{Core}(x_i))). \end{cases}$$

Definition 3. A cluster detected by the density-based algorithm DBSCAN is a maximal set of density connected instances, i.e., $C_i = \{x \in D \mid CON_\epsilon^\tau(x, c_i)\}$, where $c_i = \arg \max_{x \in C_i} \widehat{pdf}_\epsilon(x)$ is the cluster mode.

For this kind of algorithm to find all clusters in a dataset, the data distribution must have the following necessary condition: the peak density of each cluster must be greater than the maximum over all possible paths of the minimum density along any path linking any two modes.² This condition is formally described by Zhu et al³⁶ as follows:

$$\min_{k \in \{1, \dots, \varsigma\}} c_k > \max_{i \neq j \in \{1, \dots, \varsigma\}} g_{ij} \quad (2)$$

where g_{ij} is the largest of the minimum density along any path linking the mode of for clusters C_i and C_j .

This condition implies that there must exist a threshold τ that can be used to break all paths between the modes by assigning regions with density less than τ to noise. Otherwise, if the mode of some cluster has a density lower than that of a low-density region between other clusters, then this kind of density-based clustering algorithm will fail to find all clusters. Either some high-density clusters will be merged together (when a lower density threshold is used), or low-density clusters will be designated as noise (when a higher density threshold is used). To illustrate, Figure 2a shows that using a high threshold τ_1 will cause all points in Cluster C_3 to be assigned to noise but using a low threshold τ_2 will cause points in C_1 and C_2 to be assigned to the same cluster.

2.2 kNN anomaly detection

A classic nearest-neighbour based anomaly detection algorithm assigns an anomaly score to an instance based on its distance to the k -th nearest neighbour²⁷. The instances with the largest anomaly scores are identified as anomalies.

² A path linking two modes c_i and c_j is defined as a sequence of unique points starting with c_i and ending with c_j where adjacent points lie in each other's ϵ -neighbourhood.

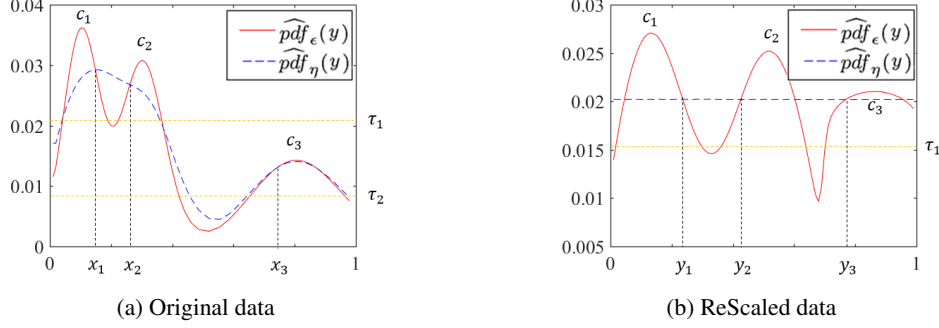


Figure 2: (a) A mixture of three Gaussian distributions that cannot be separated using a single density threshold; (b) Density distribution on ReScaled data of (a), where a single density threshold can be found to separated all three clusters. Note that point x_1, x_2 and x_3 are shifted to y_1, y_2 and y_3 , respectively. Here η is a larger bandwidth than ϵ .

Given a dataset and the parameter k , the density of x can be estimated using a k -th nearest neighbour density estimator (as used by the classic k NN anomaly detector²⁷):

$$\widehat{pdf}_{kNN}(x; k) = \widehat{pdf}(x; \epsilon_k(x)) = \frac{k}{n \times V_{\epsilon_k(x)}} \propto \left(\frac{1}{\epsilon_k(x)}\right)^d \quad (3)$$

where $\epsilon_k(x)$ is the distance between $x \in \mathbb{R}^d$ and its k -th nearest neighbour in a dataset D .

Note that the k -th nearest neighbour distance $\epsilon_k(x)$ is a proxy to the density of x , i.e., high $\epsilon_k(x)$ indicates low density, and vice versa.

Let C be the set of all normal points in a dataset D . The condition under which the classic k NN anomaly detector *could*, with an appropriate setting of a density/distance threshold, identify every anomaly y in $A = D \setminus C$ is given as follows:

$$\min_{y \in A} \epsilon_k(y) > \max_{x \in C} \epsilon_k(x) \quad (4)$$

Equation 4 states that all anomalies must have the highest k NN distances (or lowest densities) in order to detect them. In other words, k NN anomaly detectors can detect both global anomalies and scattered anomalies which have lower densities than that of all normal points^{1,20}.

However, based on this characteristic, k NN anomaly detectors are unable to detect:

- (a) Local anomalies. This is because a local anomaly y with low density relative to nearby normal (non-anomalous) instances in a region of high average density may still have higher density than that of normal (non-anomalous) instances in regions of lower average density⁷. Translating this in terms of k -th NN distance, we have: $\forall_{x,z \in C, y \in A} \epsilon_k(x) < \epsilon_k(y) < \epsilon_k(z)$. Here, some local anomalies (for example, points located around the boundaries of C_1 and C_2) are ranked lower than the normal points located around the centre sparse cluster (C_3), as shown in Figure 2a.
- (b) Anomalous clusters (sometimes referred to as clustered anomalies²¹) are groups of points that are too small to be considered “true clusters” and are found in low density parts of the space (i.e. are separate from the other clusters). A purported benefit of the k NN anomaly detector is that it is able to remove such anomalous clusters providing k is sufficiently large (larger than the size of the anomalous group)¹. By rescaling the data we are able to extend this property to locally anomalous clusters, i.e. to be tolerant to variations in the local (background or average) density over the space. An example is shown in Figure 3.

2.3 Summary

Both density-based clustering and distance-based anomaly detector have weaknesses when it comes to handling datasets with inhomogeneous density clusters. Rather than creating a new density estimator or modifying the existing clustering and anomaly detection algorithm procedures, we advocate transforming data to be more uniformly distributed than it is in the original space such that the separation between clusters can be identified easily.

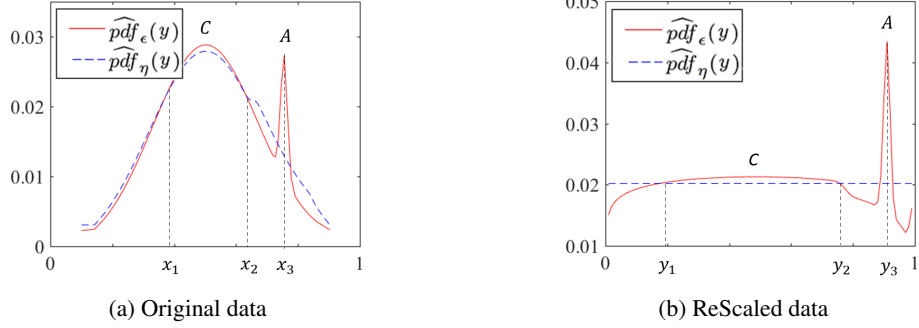


Figure 3: (a) A mixture of two Gaussian distributions that C is a normal cluster and A is an anomalous cluster; (b) Density distribution on the ReScaled data of (a), where the anomalous cluster are farther to the normal cluster centre. Note that Point x_1 , x_2 and x_3 are shifted to y_1 , y_2 and y_3 , respectively.

3 Density-ratio estimation

Density-ratio estimation is a principled approach to overcome the weakness of density-based clustering for detecting clusters with inhomogeneous densities³⁶.

The density-ratio of a point is the ratio of two density estimates calculated using the same density estimator, but with two different bandwidth settings.

Let $pdf(\cdot, \gamma)$ and $pdf(\cdot, \lambda)$ be density estimators using kernels of bandwidth γ and λ , respectively. Given the constraint that the denominator has larger bandwidth than the numerator $\gamma < \lambda$, the density ratio of x is estimated as

$$rpdf(x; \gamma, \lambda) = \frac{pdf(x; \gamma)}{pdf(x; \lambda)} \quad (5)$$

We correct the lemma from³⁶ regarding the density ratio value :

Lemma 1. *For any data distribution and sufficiently small values of γ and λ s.t. $\gamma < \lambda$, if x is at a local maximum density of $\mathcal{N}(x; \lambda)$, then $rpdf(x; \gamma, \lambda) \geq 1$; and if x is at a local minimum density of $\mathcal{N}(x; \lambda)$, then $rpdf(x; \gamma, \lambda) \leq 1$.*

Since points located at local high-density areas (almost invariably) have density-ratio higher than points located at local low-density areas, a global density-ratio threshold around unity can be used to identify all cluster peaks and break all paths between different clusters. Thus, based on density-ratio estimation, existing density-based clustering algorithms such as DBSCAN can identify clusters as regions of locally high density, separated by regions of locally low density.

Similarly, a density-based anomaly detector is able to detect local anomalies since their density-ratio values are lower and ranked higher than normal points with locally high densities.

4 CDF scaling to overcome the issue of inhomogeneous densities

4.1 One-dimensional CDF scaling

Let $pdf(\cdot, \lambda)$ and $cdf(\cdot, \lambda)$ be a density estimator and a cumulative density estimator, respectively, using a kernel of bandwidth λ .

Let x' be a transformed point of x using cdf as follows:

$$x' = cdf(x; \lambda) \quad (6)$$

Then, we have the property as follows³⁶:

$$pdf(x'; \lambda) = 1/n \quad (7)$$

and

$$pdf(x'; \gamma) \approx \frac{pdf(x; \gamma)}{pdf(x; \lambda)} \text{ for } \lambda > \gamma \quad (8)$$

ReScale³⁶ is a representative implementation algorithm based on this *cdf* transform. Figure 2b and Figure 3b show ReScale rescales the data distribution on two 1-dimensional datasets, respectively. They show that clusters and anomalies are easier to identify after the application of ReScale.

Since this *cdf* transform can be performed on a one-dimensional dataset only, ReScale must apply the transformation to each attribute independently for a multi-dimensional dataset.

4.2 Multi-dimensional CDF scaling

Using a distance scaling method, a multi-dimensional *cdf* transform can be achieved by simply rescaling the distances between each point and all the other instances in its local neighbourhood, (thereby considering all of the dimensions of the multidimensional dataset at once).

Given a point $x \in D$, the distance between x and all points in its λ -neighbourhood $y \in \mathcal{N}(x; s, \lambda)$ ³ can be rescaled using a scaling function $r(\cdot)$:

$$\forall_{x,y \in D, y \in \mathcal{N}(x; s, \lambda)} s'(x, y) = s(x, y) \times r(x; \lambda) \quad (9)$$

where $s'(\cdot, \cdot)$ is the scaled distance of $s(\cdot, \cdot)$.

Here, the scaling function $r(x; \lambda)$ depends on both the position x and size of the neighbourhood λ . It is defined as follows using the estimated density $pdf(x; s, \lambda)$ with the aim of making the density distribution within the λ -neighbourhood uniform:

$$r(x; \lambda) = \frac{m}{\lambda} \times \left(\frac{pdf(x; s, \lambda) \times V_\lambda}{n} \right)^{\frac{1}{d}} \propto pdf(x; s, \lambda)^{\frac{1}{d}} \quad (10)$$

where $m = \max_{x,y \in D} s(x, y)$ is the maximum pairwise distance in D . Note that we have now reparameterised the density estimator $pdf(x; s, \lambda)$ to include the distance function s , in order to facilitate calculations below.

With reference to the uniform distribution which has density $\frac{n}{V_m}$, where V_m is the volume of the ball having radius m :

$$r(x; \lambda) < 1 \text{ if } pdf(x; s, \lambda) < \frac{n}{V_m} \quad (11)$$

$$r(x; \lambda) > 1 \text{ if } pdf(x; s, \lambda) > \frac{n}{V_m} \quad (12)$$

That is, the process rescales sparse regions to be more dense by using $r(x; \lambda) < 1$, and dense regions to be more sparse by using $r(x; \lambda) > 1$; such that the entire dataset is approximately uniformly distributed in the scaled λ -neighbourhood. More specifically, after rescaling distances with s' , the density of points in the neighbourhood of size $\lambda'_x = \lambda \times r(x; \lambda)$ around x is the same as the density of points across the whole dataset:

$$\begin{aligned} pdf(x; s', \lambda'_x) &= \frac{pdf(x; s, \lambda) \times V_\lambda}{V_{\lambda'_x}} = \frac{pdf(x; s, \lambda) \times V_\lambda}{V_\lambda \times r(x; \lambda)^d} \\ &= \frac{pdf(x; s, \lambda) \times V_\lambda}{V_\lambda \times \left(\frac{m}{\lambda} \times \left(\frac{pdf(x; s, \lambda) \times V_\lambda}{n} \right)^{\frac{1}{d}} \right)^d} = \frac{n \times \lambda^d}{V_\lambda \times m^d} = \frac{n}{V_m} \end{aligned} \quad (13)$$

Note that the above derivation is possible because (i) the scaling is isotropic about x (hence the shape of the unit ball doesn't change only its size) and (ii) the uniform-kernel density estimator is local (i.e., its value depends only on points within the λ'_x neighbourhood).

In order to maintain the same relative ordering of distances between x and all other points in the dataset, the distance between x and any point not in the λ -neighbourhood $y \in D \setminus \mathcal{N}(x; s, \lambda)$ can be normalised by a simple *min-max* normalisation:

$$\forall_{y \in D \setminus \mathcal{N}(x; s, \lambda)} s'(x, y) = (s(x, y) - \lambda) \times \frac{m - \lambda'_x}{m - \lambda} + \lambda'_x \quad (14)$$

³For reasons that will become obvious shortly, we now reparameterise the neighbourhood function $\mathcal{N}(x; s, \lambda)$ to depend on the distance measure s .

It is interesting to note that providing λ is sufficiently large that the average of the density estimates across the data points approximates the average density over the space $\mathbb{E}_{x \in D}[\text{pdf}(x; s, \lambda)] \approx \frac{n}{V_m}$, then we have that the average rescaling factor is approximately 1: $\mathbb{E}_{x \in D}[r(x; \lambda)] \approx 1$, $\mathbb{E}_{x \in D}[\lambda'_x] \approx \lambda$, and thus the average distance between points is unchanged after rescaling.⁴

$$\forall_{y \in D} \quad \mathbb{E}_{x \in D}[s'(x, y)] \approx \mathbb{E}_{x \in D}[s(x, y)] \quad (15)$$

The implementation of DScale³⁷, which is a representative algorithm based on this multi-dimensional CDF scaling, is provided in Algorithm 2 in Appendix 8.

A lemma about the density on the rescaled distance is given as follows:

Lemma 2. *The density $\text{pdf}(x; s', \gamma'_x)$ with the rescaled distance s' is approximately proportional to the density-ratio $\frac{\text{pdf}(x; s, \gamma)}{\text{pdf}(x; s, \lambda)}$ in terms of the original distance s within the λ -neighbourhood of x .*

Proof.

$$\begin{aligned} \text{pdf}(x; s', \gamma'_x) &\approx \frac{\text{pdf}(x; s, \gamma) \times V_\gamma}{V_{\gamma'_x}} = \frac{\text{pdf}(x; s, \gamma) \times V_\gamma}{V_\gamma \times r(x; \lambda)^d} \\ &= \frac{\text{pdf}(x; s, \gamma)}{\frac{m^d}{\lambda^d} \times \frac{\text{pdf}(x; s, \lambda) \times V_\lambda}{n}} = \frac{n}{V_m} \times \frac{\text{pdf}(x; s, \gamma)}{\text{pdf}(x; s, \lambda)} \\ &\propto \frac{\text{pdf}(x; s, \gamma)}{\text{pdf}(x; s, \lambda)} \end{aligned}$$

where $\gamma'_x = \gamma \times r(x; \lambda)$ and $\gamma < \lambda$. \square

Note that the above lemma is only valid within the λ -neighbourhood of x , and when each $x \in D$ is treated independently. In other words, the *cdf* transform is only valid locally. In addition, the rescaled distance is asymmetric, i.e., $s'(x, y) \neq s'(y, x)$ when $r(x; \lambda) \neq r(y; \lambda)$.

To be a valid *cdf* transform globally for the entire dataset, we propose in this paper to perform an iterative process that involves two steps: distance rescaling and point shifting.

5 CDF Transform-Shift (CDF-TS)

Instead of just rescaling distances between each data instance x and all other points in the dataset, we can apply the rescaling directly to the dataset by translating points in approximate accordance with the rescaled distances. Two advantages of the new approach are: (i) the shifted dataset becomes approximately uniformly distributed as a whole; and (ii) the standard Euclidean distance can then be used to measure distances between the transformed points, rather than the non-symmetric and as a result non-metric rescaled distance.

Consider two points $x, y \in D$. In order to make the distribution around point x more uniform, we wish to rescale (expand or contract) the distance between x and y to be $s'(x, y)$ as defined by Equations 9 and 14. We can do this by translating the point y to a new point denoted y'_x which lies along the direction $(y - x)$ as follows:

$$y'_x = x + \frac{s'(x, y)}{s(x, y)}(y - x) \quad (16)$$

Note that the distance between x and the newly transformed point y'_x satisfies the rescaled distance requirement:

$$s(x, y'_x) = s'(x, y) \quad (17)$$

Above we considered the effect of translating point y to y'_x to scale the space around point x . In order to approximately scale the space around all points in the dataset, point y needs to be translated by the average of the above translations:

$$\bar{y}' = \frac{1}{n} \sum_{x \in D} y'_x = \frac{1}{n} \sum_{x \in D} x + \frac{s'(x, y)}{s(x, y)}(y - x) \quad (18)$$

A theorem regarding the final shifted data D' is provided as follows:

⁴Proof: For $y \in \mathcal{N}(x, s, \lambda)$ we have that $\mathbb{E}_{x \in D}[s'(x, y)] \approx \mathbb{E}_{x \in D}[r(x; \lambda)]\mathbb{E}_{x \in D}[s(x, y)] \approx \mathbb{E}_{x \in D}[s(x, y)]$ since $r(x; \lambda)$ and $s(x, y)$ are independent. The same can be shown for points $y \notin \mathcal{N}(x, s, \lambda)$.

Theorem 1. Given a sufficiently large bandwidth $\lambda < m$, the λ -neighbourhood density of D' is expected to be more uniform than that of D :

$$\forall_{x \in D} |pdf(\bar{x}'; s, \lambda) - n/V_m| < |pdf(x; s, \lambda) - n/V_m|,$$

Proof. Let us define the bandwidth $\bar{\lambda}'_x$ for the transformed neighbourhood around \bar{x}' as $\bar{\lambda}'_x = \lambda \times \frac{s(\bar{x}', \bar{y}')}{s(x, y)}$ where $x, y \in D$ and $y \in \mathcal{N}(x, s, \lambda)$. We can now estimate $\bar{\lambda}'_x$ as follows. We have

$$\begin{aligned} s(\bar{x}', \bar{y}') &= \|\bar{x}' - \bar{y}'\| \\ &= \left\| \frac{1}{n} \sum_{z \in D} \left(\frac{s'(z, x)}{s(z, x)} (x - z) - \frac{s'(z, y)}{s(z, y)} (y - z) \right) \right\| \end{aligned}$$

Since y is in the λ -neighbourhood of x we have $\forall_{z \in D} \frac{s'(z, x)}{s(z, x)} \approx \frac{s'(z, y)}{s(z, y)}$, and

$$\begin{aligned} s(\bar{x}', \bar{y}') &\approx \left\| \frac{1}{n} \sum_{z \in D} \frac{s'(z, x)}{s(z, x)} (x - z) \right\| \\ &= s(x, y) \frac{1}{n} \sum_{z \in D} \frac{s'(z, x)}{s(z, x)} \\ \frac{s(\bar{x}', \bar{y}')}{s(x, y)} &= \frac{1}{n} \left(\sum_{z \in \mathcal{N}(x; s, \lambda)} \frac{s'(z, x)}{s(z, x)} + \sum_{z \notin \mathcal{N}(x; s, \lambda)} \frac{s'(z, x)}{s(z, x)} \right) \end{aligned}$$

Supposing that $pdf(z; s, \lambda)$ varies slowly within the neighbourhood $\mathcal{N}(x; s, \lambda)$, we have:

$$\sum_{z \in \mathcal{N}(x; s, \lambda)} \frac{s'(z, x)}{s(z, x)} \approx \sum_{z \in \mathcal{N}(x; s, \lambda)} \frac{s'(x, z)}{s(x, z)} = \sum_{z \in \mathcal{N}(x; s, \lambda)} r(x; \lambda)$$

Then based on Equation 15, given a sufficiently large λ such that $\mathbb{E}_{z \in D} [pdf(z; s, \lambda)] \approx \frac{n}{V_m}$ and providing the count $|\mathcal{N}(x; s, \lambda)|$ is sufficiently small, we have:

$$\mathbb{E}_{z, x \in D, z \notin \mathcal{N}(x; s, \lambda)} [s'(z, x)] \approx \mathbb{E}_{z, x \in D} [s'(z, x)] \approx \mathbb{E}_{z, x \in D} [s(z, x)]$$

This means that $s(\bar{x}', \bar{y}')$ is mainly affected by the point z located in the λ -neighbourhood of x , i.e., $\mathbb{E}_{z, x \in D, z \notin \mathcal{N}(x; s, \lambda)} \left[\frac{s'(z, x)}{s(z, x)} \right] \approx 1$. Then we have

$$\begin{aligned} \frac{s(\bar{x}', \bar{y}')}{s(x, y)} &\approx \frac{1}{n} \left(\sum_{z \in \mathcal{N}(x; s, \lambda)} r(x; \lambda) + \sum_{z \notin \mathcal{N}(x; s, \lambda)} 1 \right) \\ &= \left(\frac{|\mathcal{N}(x; s, \lambda)|}{n} \times r(x; \lambda) + \frac{n - |\mathcal{N}(x; s, \lambda)|}{n} \right) \end{aligned}$$

The above relation can be rewritten as:

$$\frac{\frac{s(\bar{x}', \bar{y}')}{s(x, y)} - 1}{r(x; \lambda) - 1} \approx \frac{|\mathcal{N}(x; s, \lambda)|}{n}$$

As $\frac{|\mathcal{N}(x; s, \lambda)|}{n} \in (0, 1)$, the relation between $\frac{s(\bar{x}', \bar{y}')}{s(x, y)}$ and $r(x; \lambda)$ depends on whether x is in the sparse or dense region:

$$r(x; \lambda) < \frac{s(\bar{x}', \bar{y}')}{s(x, y)} < 1 \text{ if } pdf(x; s, \lambda) < \frac{n}{V_m} \quad (19)$$

$$r(x; \lambda) > \frac{s(\bar{x}', \bar{y}')}{s(x, y)} > 1 \text{ if } pdf(x; s, \lambda) > \frac{n}{V_m} \quad (20)$$

When the density varies slowly in the $\mathcal{N}(x; s, \lambda)$, we can safely assume that each point's nearest neighbours keep similar after transform and the density still varied slowly in $\bar{\lambda}'$ -neighbourhood. Then we have $\mathbb{E}_{x \in D} \mathcal{N}(x'; s, \bar{\lambda}') \approx \mathcal{N}(x; s, \lambda)$ and $pdf(\bar{x}'; s, \lambda)$ can estimate as

$$\begin{aligned}
pdf(\bar{x}'; s, \lambda) &\approx pdf(\bar{x}'; s, \bar{\lambda}') \\
&\approx \frac{|\mathcal{N}(x; s, \lambda)|}{V_{\lambda'}} = \frac{pdf(x; s, \lambda) \times V_{\lambda}}{V_{\lambda} \times (\frac{s(\bar{x}', \bar{y}')}{s(x, y)})^d}
\end{aligned} \tag{21}$$

Here we have three scenarios, depending on the density of x :

1. In sparse region $pdf(x; s, \lambda) < n/V_m$, we have $r(x; \lambda) < \frac{s(\bar{x}', \bar{y}')}{s(x, y)} < 1$, as shown in Equation 19. Using this inequality in Equations 13 and 21, we have

$$n/V_m > pdf(\bar{x}'; s, \lambda) > pdf(x; s, \lambda)$$

2. In dense region $pdf(x; s, \lambda) > n/V_m$, we have $r(x; \lambda) > \frac{s(\bar{x}', \bar{y}')}{s(x, y)} > 1$, as shown in Equation 20. Using this inequality in Equations 13 and 21, we have

$$n/V_m < pdf(\bar{x}'; s, \lambda) < pdf(x; s, \lambda)$$

Therefore, $\forall_{x \in D}, |pdf(\bar{x}'; s, \lambda) - n/V_m| < |pdf(x; s, \lambda) - n/V_m|$. \square

Since our target is to get a uniformly distributed data w.r.t. $pdf(\bar{x}', s, \lambda)$, this transform-shift process can be repeated multiple times using an iterative method to reduce the λ -neighbourhood density variation on the shifted dataset in the previous iteration.

This is accomplished by using an expectation-maximisation-like algorithm. The objective is to minimise the density variance in D' .

A condition for terminating the iteration process is when the total distance of point-shifts from D to D' in the latest iteration is less than a threshold δ , i.e.,

$$\sum_{x \in D, \bar{x}' \in D'} |x - \bar{x}'| \leq \delta \tag{22}$$

Note that, due to the shifts in each iteration, the value ranges of attributes of the shifted dataset D' are likely to be different from those of the original dataset D . We can use a min-max normalisation³ on each attribute to keep the values in the same fixed range at the end of each iteration.

Figure 4 illustrates the effects of CDF-TS on a two-dimensional data with different iterations. It shows that the original clusters with different density become increasing uniform as the number of iterations increases.

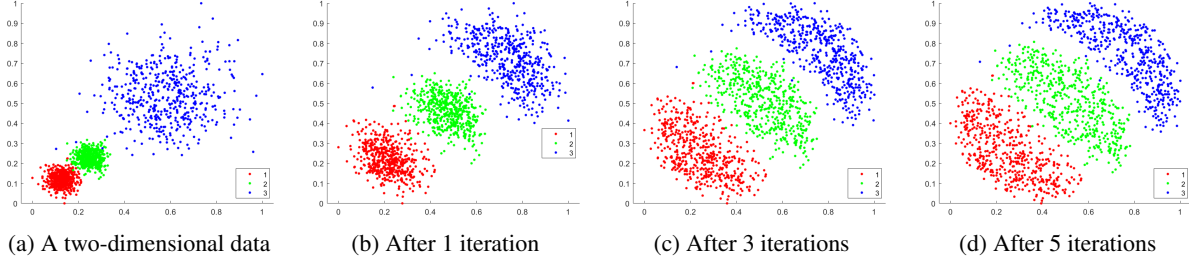


Figure 4: Illustrating the effects of CDF-TS on a two-dimensional data with $\lambda = 0.1$.

The implementation of CDF-TS is shown in Algorithm 1. The DScale algorithm used in step 6 is provided in Algorithm 2 in Appendix 8. Algorithm 1 requires two parameters λ and δ .

Algorithm 1 CDF-TS(D, λ, δ)

Input: D - input data matrix ($n \times d$ matrix); λ - bandwidth parameter; δ - threshold for the total shifted distance.**Output:** D' - data matrix after rescaling and point shifting.

```

1: Normalising  $D$  using min-max normalisation
2:  $\Delta = \infty$ 
3:  $t = 1$ 
4: while  $\Delta > \delta$  do
5:    $S \leftarrow$  Calculating the distance matrix for  $D$ 
6:    $S' \leftarrow \text{DScale}(S, \lambda, d)$ 
7:   for each  $z \in D$  (where  $z$  is a reference point) do
8:      $D_z \leftarrow$  Shift every point  $x \in D$  to  $x'_z$  in the direction of  $z$  to  $x$  with magnitude  $S'[z, x]$ 
9:   end for
10:   $D' \leftarrow \frac{1}{n} \sum_{z \in D} D_z$ 
11:  Normalising  $D'$  using min-max normalisation
12:   $\Delta = \frac{1}{nd} \sum_{i,j} |D[i, j] - D'[i, j]|$ 
13:   $t = t + 1$ 
14:   $D = D'$ 
15: end while
16: return  $D'$ 

```

5.1 Density estimators applicable to CDF-TS

The following two types of density estimators, with fixed-size and variable-size bandwidths of the uniform kernel, are applicable to CDF-TS to do the CDF scaling:

(a) ϵ -neighbourhood density estimator:

$$\widehat{pdf}_\epsilon(x) = \frac{|\{y \in D \mid s(x, y) \leq \epsilon\}|}{nV_\epsilon}$$

where V_ϵ is the volume of the ball with radius ϵ .

When this density estimator is used in CDF-TS, the λ -neighbourhood described in Sections 4.2 and 5, i.e., $\mathcal{N}(x; s, \lambda) = \{y \in D \mid s(x, y) \leq \epsilon\}$, where $\lambda = \epsilon$, denoting the fixed-size bandwidth uniform kernel.

(b) k -th nearest neighbour density estimator:

$$\widehat{pdf}(x; \epsilon_k(x)) = \frac{k}{nV_{s(x, x_k)}} \propto \left(\frac{1}{s(x, x_k)}\right)^d$$

where x_k is the k -th nearest neighbour of x ; $\epsilon_k(x)$ is k -th nearest neighbour distance of x .

When this density estimator is used in CDF-TS, the neighbourhood size λ becomes dependent on the location x and the distribution of surrounding points. We denote $\lambda(x)_k = s(x, x_k)$ as the distance to the k 'th nearest neighbour of x . In this case the density is simply calculated over the neighbourhood: $\mathcal{N}(x; s, \lambda(x)_k) = \{y \in D \mid s(x, y) \leq s(x, x_k)\}$, denoting the variable-size bandwidth uniform kernel, i.e., small in dense region and large in sparse region. Note that, in this circumstance, the density of the shifted points still become more uniformly w.r.t their surrounding.

In the following experiments, we employ the same density estimators as used in DBSCAB and DP (in clustering) and kNN anomaly detector in CDF-TS to transform D to D' , i.e., ϵ -neighbourhood density estimator is used in CDF-TS for clustering; and k -th nearest neighbour density estimator is used in CDF-TS for anomaly detection.

6 Empirical Evaluation

This section presents experiments designed to evaluate the effectiveness of CDF-TS.

All algorithms used in our experiments were implemented in Matlab R2017a (the source code can be obtained at <https://sourceforge.net/p/cdf-ts/>). The experiments are run on a machine with eight cores CPU (Intel Core i7-7820X @ 3.60GHz), 32GB memory and a 2560 CUDA cores GPU (GeForce GTX 1080). All datasets were normalised using the *min-max* normalisation to yield each attribute to be in [0,1] before the experiments began.

Table 2: Properties of clustering datasets

Dataset	Data Size	#Dimensions	#Clusters
Segment	2310	19	7
Mice	1080	83	8
Biodeg	1055	41	2
ILPD	579	9	2
ForestType	523	27	4
Wilt	500	5	2
Musk	476	166	2
Libras	360	90	15
Dermatology	358	34	6
Ecoli	336	7	8
Haberman	306	3	2
Seeds	210	7	3
Lung	203	3312	5
Wine	178	13	3
3L	560	2	3
4C	1250	2	4

For clustering, we used 2 artificial datasets and 14 real-world datasets with different data sizes and dimensions from UCI Machine Learning Repository¹¹. Table 2 presents the data properties of the datasets. 3L is a 2-dimensional data containing three elongated clusters with different densities, as shown in Figure 5a. 4C is a 2-dimensional dataset containing four clusters with different densities (three Gaussian clusters and one elongated cluster), as shown in Figure 5b. Note that DBSCAN is unable to correctly identify all clusters in both of these datasets because they do not satisfy the condition specified in Equation 2. Furthermore, clusters in 3L significantly overlap on individual attribute projections, which violates the requirement of ReScale that the one-dimensional projections allow for the identification of the density peaks of each cluster.

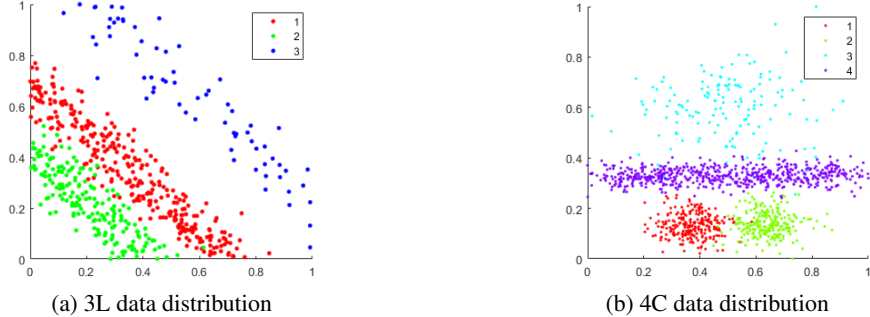


Figure 5: (a) A two-dimensional data containing three elongated clusters. (b) A two-dimensional data containing four clusters.

For anomaly detection, we compared the anomaly detection performance on 2 synthetic datasets with anomalous clusters and 10 real-world benchmark datasets⁵. The data size, dimensions and percentage of anomalies are shown in Table 3. Both the Syn 1 and Syn 2 datasets contain clusters of anomalies. Their data distributions are shown in Figure 6.

6.1 Clustering

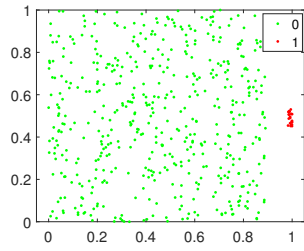
In this section, we compare CDF-TS with ReScale and DScale using two existing density-based clustering algorithms, i.e., DBSCAN¹⁴ and DP²⁹, in terms of F-measure²⁸: given a clustering result, we calculate the precision score P_i and the recall score R_i for each cluster C_i based on the confusion matrix, and then the F-measure score of C_i is the harmonic mean of P_i and R_i . The overall F-measure score is the unweighted (macro) average over all clusters: $\text{F-measure} = \frac{1}{s} \sum_{i=1}^s \frac{2P_iR_i}{P_i+R_i}$ ⁶.

⁵Velocity, Ant and Tomcat are from <http://opencosmics.us/repo/defect/ck/> and others are from UCI Machine Learning Repository¹¹.

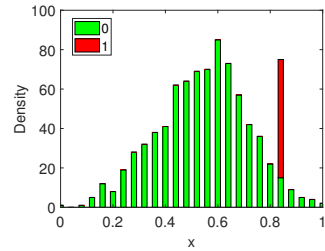
⁶It is worth noting that other evaluation measures such as purity and Normalised Mutual Information (NMI)³¹ only take into account the points assigned to clusters and do not account for noise. A clustering algorithm which assigns the majority of the points

Table 3: Properties of anomaly detection datasets

Dataset	Data Size	#Dimensions	% Anomaly
AnnThyroid	7200	6	7.42%
Pageblocks	5473	10	10.23%
Tomcat	858	20	8.97%
Ant	745	20	22.28%
BloodDonation	604	4	5.63%
Vowel	528	10	9.09%
Mfeat	410	649	2.44%
Dermatology	366	20	5.46%
Balance	302	4	4.64%
Velocity	229	20	34.06%
Syn 1	520	2	3.85%
Syn 2	860	1	6.98%



(a) Data distribution on Syn 1 dataset



(b) Stacked histogram on Syn 2 dataset

Figure 6: Data distributions of the Syn 1 and Syn 2 datasets, where the red colour indicate the anomaly.

We report the best clustering performance after performing a parameter search for each algorithm. Table 4 lists the parameters and their search ranges for each algorithm. ψ in ReScale controls the precision of $\widehat{cdf}_\lambda(x)$, i.e., the number of intervals used for estimating $\widehat{cdf}_\lambda(x)$. We set $\delta = 0.015$ as the default value for CDF-TS.

Table 4: Parameters and their search range. The search ranges of ψ and λ are as used by Zhu et. al.³⁶.

Algorithm	Parameter with search range
DBSCAN	$Minpts \in \{2, 3, \dots, 10\}; \epsilon \in [0, 1]$
DP	$k \in \{2, 3, \dots, 10\}; \epsilon \in [0, 1]$
ReScale	$\psi = 100; \lambda \in \{0.1, 0.2, \dots, 0.5\}$
DScale	$\lambda \in \{0.1, 0.2, \dots, 0.5\}$
CDF-TS	$\lambda \in \{0.1, 0.2, \dots, 0.5\}; \delta = 0.015$

Table 5 shows the best F-measures for DBSCAN, DP, their ReScale, DScale and CDF-TS versions. The average F-measures, showed in the second-to-last row, reveal that CDF-TS improves the clustering performance of either DBSCAN or DP with a larger performance gap than both ReScale and DScale. In addition, CDF-TS is the best performer on many more datasets than other contenders (shown in the last row of Table 5.).

It is interesting to see that CDF-TS exhibits a large performance improvement over both DBSCAN and DP on many datasets, such as ForestType, Wilt, Dermatology, Ecoli, Lung and Wine. On many of these datasets, CDF-TS also shows a large performance gap in comparison with ReScale and/or DScale.

Note that the performance gap is smaller for DP than it is for DBSCAN because DP is a more powerful algorithm which does not rely on a single density threshold to identify clusters.

To evaluate whether the performance difference among the three scaling algorithms is significant, we conduct the Friedman test with the post-hoc Nemenyi test¹⁰.

to noise may result in a high clustering performance. Thus the F-measure is more suitable than purity or NMI in assessing the clustering performance of density-based clustering.

Table 5: Best F-measure of DBSCAN, DP, and their ReScale, DScale and CDF-TS versions. For each clustering algorithm, the best performer in each dataset is boldfaced. Ori, ReS, and DS represent the Original algorithm, ReScale, and DScale respectively.

Data	DBSCAN				DP			
	Orig	ReS	DS	CDF-TS	Orig	ReS	DS	CDF-TS
Segment	0.59	0.62	0.61	0.67	0.78	0.77	0.80	0.84
Mice	0.99	0.99	0.99	0.993	1.00	1.00	1.00	1.00
Biodeg	0.45	0.44	0.47	0.52	0.72	0.74	0.73	0.76
ILPD	0.41	0.42	0.56	0.52	0.60	0.63	0.62	0.64
ForestType	0.27	0.51	0.48	0.65	0.69	0.83	0.70	0.85
Wilt	0.38	0.39	0.54	0.55	0.54	0.68	0.54	0.74
Musk	0.51	0.52	0.51	0.53	0.55	0.58	0.61	0.62
Libras	0.41	0.44	0.46	0.49	0.376	0.375	0.376	0.38
Dermatology	0.52	0.73	0.74	0.83	0.91	0.97	0.91	0.96
Ecoli	0.37	0.40	0.54	0.60	0.48	0.55	0.63	0.64
Haberman	0.47	0.64	0.59	0.66	0.56	0.63	0.58	0.67
Seeds	0.75	0.88	0.85	0.83	0.91	0.92	0.92	0.94
Lung	0.49	0.54	0.49	0.66	0.70	0.74	0.64	0.72
Wine	0.64	0.86	0.80	0.90	0.93	0.95	0.96	0.962
3L	0.59	0.63	0.90	0.88	0.82	0.81	0.86	0.89
4C	0.71	0.90	0.92	0.95	0.87	0.92	0.95	0.91
Average	0.53	0.62	0.65	0.70	0.72	0.75	0.74	0.78
#Top 1	0	1	2	13	1	3	2	13

Figures 7a and 7b show the results of the significance test for DBSCAN and DP, respectively. The results show that the CDF-TS versions are significantly better than the DScale and ReScale versions for both DBSCAN and DP.

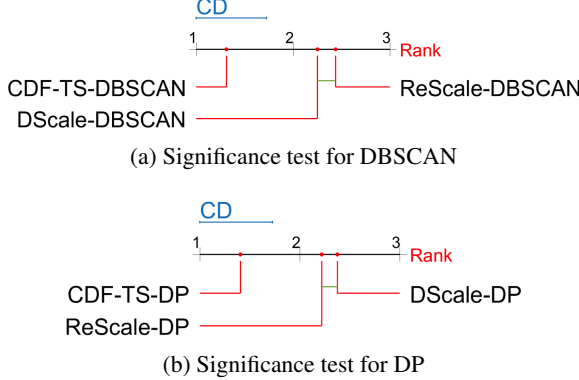


Figure 7: Critical difference (CD) diagram of the post-hoc Nemenyi test ($\alpha = 0.10$). Two algorithms are significant different if the gap between their ranks is larger than CD. Otherwise, there is a line linking them.

Here we compare the different effects on the transformed datasets due to ReScale and CDF-TS using the MDS visualisation⁷.

The effects on the two synthetic datasets are shown in Figure 8 and Figure 9. They show that both the rescaled datasets are more axis-parallel distributed using ReScale than those using CDF-TS. For the 3L dataset, the blue cluster is still very sparse after running ReScale, as shown in Figure 8a. In contrast, it becomes denser using CDF-TS, as shown in Figure 9a. As a result, DBSCAN has much better performance with CDF-TS on the 3L dataset.

⁷Multidimensional scaling (MDS)⁶ is used for visualising a high-dimensional dataset in a 2-dimensional space through a projection method which preserves as well as possible the original pairwise dissimilarities between instances.

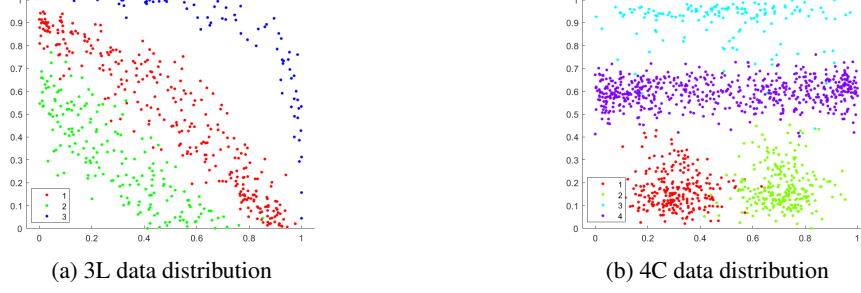


Figure 8: Data distribution after running ReScale when achieving the best DBSCAN clustering performance

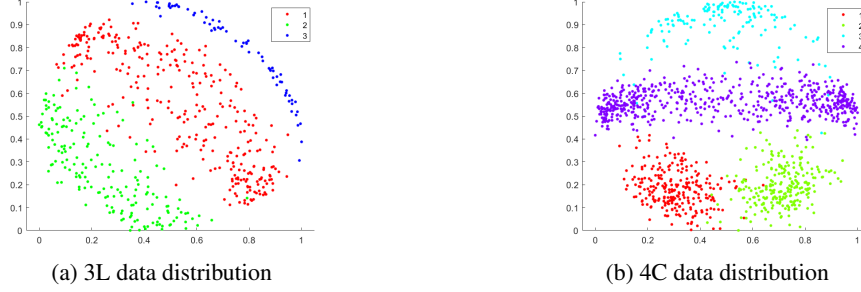


Figure 9: Data distribution after running CDF-TS when achieving the best DBSCAN clustering performance

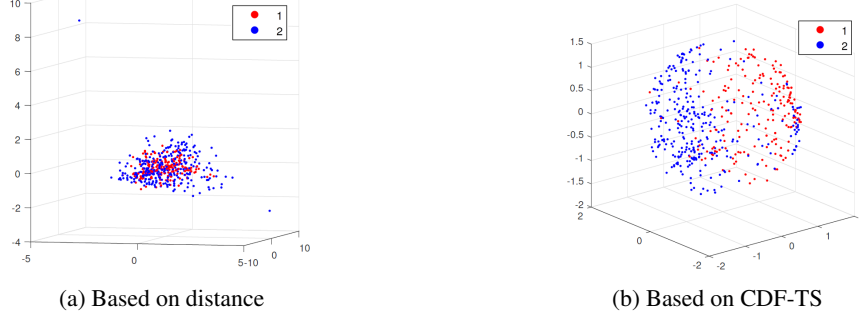


Figure 10: MDS plots on the Wilt dataset

Figure 10 shows the MDS plots on the Wilt dataset which CDF-TS has the largest performance improvement over both DBSCAN and DP. The figure shows that the two clusters are more uniformly distributed in the new space which makes their boundary easier to be identified than that in the original space. In contrast, based on distance, most points of the red cluster are surrounded by points of the blue cluster, as shown in Figure 10a.

6.2 Anomaly detection

In this section, we evaluate the ability of CDF-TS to detect local anomalies based on k NN anomaly detection.

Two state-of-the-art local anomaly detector, Local Outlier Factor (LOF)⁷ and iForest^{19,22}, are also used in the comparison. Table 6 lists the parameters and their search ranges for each algorithm. Parameters ψ and t in iForest control the sub-sample size and number of iTrees, respectively. We report the best performance of each algorithm on each dataset in terms of best AUC (Area under the Curve of ROC)¹⁵.

Table 7 compares the best AUC score of each algorithm. CDF-TS- k NN achieves the highest average AUC of 0.90 and performs the best on 6 out of 12 datasets. For the Syn 1 dataset which has overlapping on the individual attribute projection, DScale and CDF-TS have much better results than ReScale.

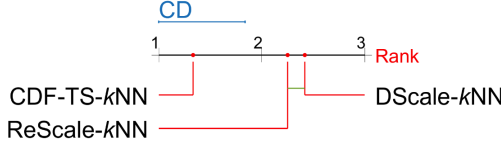
Figure 11 shows the significance test on the three algorithms applied to k NN anomaly detector. It can be seen from the results that CDF-TS- k NN is significantly better than DScale- k NN and ReScale- k NN.

Table 6: Parameters and their search ranges.

Algorithm	Parameters and their search range
<i>k</i> NN/LOF	$k \in \{5\%n, 10\%n, \dots, 50\%n\}$
iForest	$t = 100; \psi \in \{2^1, 2^2, \dots, 2^{10}\}$
ReScale	$\psi = 100; \lambda \in \{0.1, 0.2, \dots, 0.5\}$
DScale	$\lambda \in \{0.1, 0.2, \dots, 0.5\}$
CDF-TS	$\lambda \in \{0.1, 0.2, \dots, 0.5\}; \delta = 0.015$

Table 7: Best AUC on 12 datasets. The best performer on each dataset is boldfaced. ReS, and DS represent ReScale-*k*NN, and DScale-*k*NN respectively.

Data	<i>k</i> NN	LOF	iForest	Res	DS	CDF-TS
AnnThyroid	0.65	0.68	0.88	0.76	0.71	0.94
Pageblocks	0.89	0.93	0.90	0.88	0.86	0.94
Tomcat	0.63	0.67	0.81	0.77	0.69	0.78
Ant	0.67	0.68	0.77	0.76	0.71	0.76
BloodDonation	0.69	0.79	0.82	0.84	0.80	0.86
Vowel	0.93	0.93	0.92	0.932	0.90	0.94
Mfeat	0.99	0.98	0.98	0.99	1.00	0.99
Dermatology	0.91	0.99	0.86	0.99	0.96	1.00
Balance	0.94	0.95	0.91	0.91	0.83	0.92
Velocity	0.66	0.62	0.65	0.67	0.694	0.69
Syn 1	0.92	0.93	0.90	0.89	0.95	0.98
Syn 2	0.88	0.88	0.86	0.92	0.95	0.94
Average	0.81	0.83	0.86	0.86	0.84	0.90
#Top 1	0	1	2	1	3	6

Figure 11: Critical difference (CD) diagram of the post-hoc Nemenyi test ($\alpha = 0.10$) for anomaly detection algorithms.

It is interesting to mention that CDF-TS-*k*NN has the largest AUC improvement over *k*NN on Dermatology and AnnThyroid, shown in Table 7. Table 8 compares their MDS plots between the original datasets and the shifted (density equalised) datasets. It shows that most anomalies become anomalous clusters and farther away from normal points on the shifted datasets, making them easier to detect by *k*NN anomaly detector. Note that some anomalies are closed to normal clusters and have higher densities than many normal instances in the original dataset.

6.3 Run-time

ReScale, DScale and CDF-TS are all pre-processing methods, their computational complexities are shown in Table 9. Because many existing density-based clustering algorithms have time and space complexities of $\mathcal{O}(n^2)$, all these methods does not increase their overall complexities.

Table 10 shows the runtime of the dissimilarity matrix calculation for each of the three methods on the Mfeat, Segment, Pageblocks and AnnThyroid datasets. Their parameters are set to be the same for all datasets, i.e., $\lambda = 0.2$, $\psi = 100$ and $\delta = 0.015$. The result shows that CDF-TS took the longest runtime because it requires multiple DScale calculations.

Table 8: MDS plots on two datasets, where red points indicate anomalies.

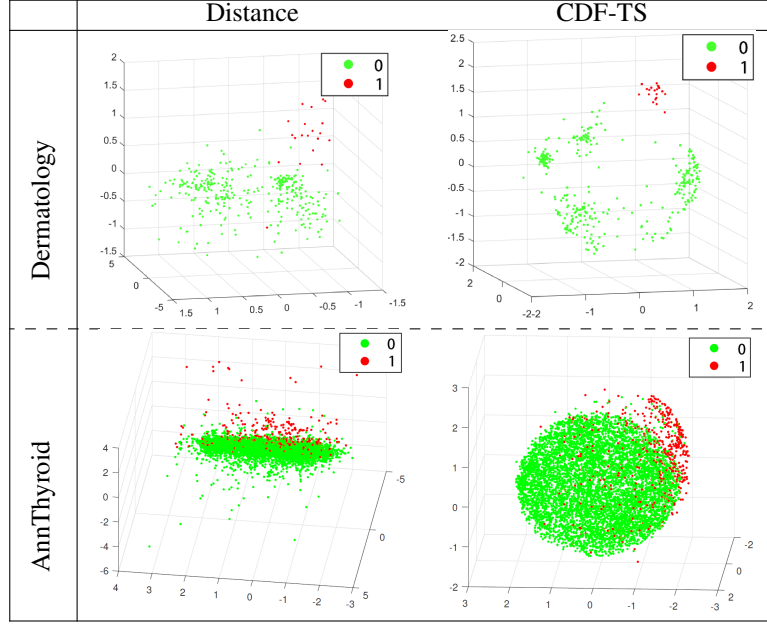


Table 9: Computational complexity of ReScale, DScale and CDF-TS.

Algorithm	Time complexity	Space complexity
ReScale	$\mathcal{O}(dn\psi)$	$\mathcal{O}(dn + d\psi)$
DScale and CDF-TS	$\mathcal{O}(dn^2)$	$\mathcal{O}(dn + n^2)$

Table 10: Runtime comparison of dissimilarity matrix calculation (in seconds).

Dataset	CPU			GPU		
	ReScale	DScale	CDF-TS	ReScale	DScale	CDF-TS
Mfeat	0.69	0.03	1.26	0.05	0.02	2.89
Segment	0.29	0.28	2.68	0.02	0.05	0.11
Pageblocks	0.16	1.64	18.64	0.02	0.17	2.84
AnnThyroid	0.19	3.09	24.40	0.02	0.26	2.97

7 Discussion

7.1 Parameter sensitivity

Both DScale and CDF-TS have one critical parameter λ to define the λ -neighbourhood. The density-ratio based on a small λ will approximate 1 and provides no information; while on a large λ will approximate the estimated density and have no advantage. Generally, $\lambda \in [0.1, 0.2]$ and ϵ in DBSCAN and DP shall be set slightly smaller than λ .

The parameter δ in CDF-TS controls the number of iterations, i.e., a smaller δ usually results in a higher number of iterations in the CDF-TS process, and makes the shifted dataset more uniform. In our experiments, we set $\delta = 0.015$ as default value and got significantly better results than existing algorithms. When tuning the best δ for different datasets, CDF-TS would get better results on most datasets.

7.2 Relation to LOF

LOF⁷ is a local density-based approach for anomaly detection. The LOF score of x is the ratio of the density of x to the average density of x 's k -nearest neighbours, where the density of x is inversely proportional to the average distance to its k -nearest-neighbours⁷.

Though LOF is a density-ratio approach, it does not employ CDF transform, which is the core technique in CDF-TS. While LOF has the ability to detect local anomalies, it is weaker in identifying anomalous clusters than k NN which employs CDF-TS.

7.3 Relation to metric learning

There are many unsupervised distance metric learning algorithms which transform data e.g., global methods such as PCA¹⁸, KPCA³⁰ and KUMMP³⁵); and local methods such as Isomap³³, t-SNE²⁴ and LPP¹⁷. These methods are usually used as dimension reduction methods such that data clusters in the learned low-dimensional space are adjusted based on some objective function³⁴.

CDF-TS is an unsupervised algorithm based on the CDF transform such that the data are more uniform in the scaled space. Though it is a linear and local method, CDF-TS is not a metric learning method for dimension reduction.

We have examined the performance of t-SNE in density-based clustering and k NN anomaly detection. We set the dimensionality of its output space to be the same as the original data. We found that t-SNE has inconsistent clustering performance. For example, while it produced the best clustering results on some high-dimensional datasets such as the ForestType and Lung datasets; but it yielded the worst results on the Breast and 3L datasets. In addition, t-SNE could not improve the performance on k NN anomaly detector. This is because anomalies are still dense or close to some dense clusters in the t-SNE transformed space.

7.4 Comparison with a density equalisation method

In the context of kernel k -means²⁵, k NN kernel²⁶ has been suggested to be a way to equalise the density of a given dataset to reduce the bias of kernel k -means algorithm and to improve the clustering performance on datasets with inhomogeneous densities. The dissimilarity matrix generated by k NN kernel is a binary matrix can be seen as the adjacent matrix of k NN graph such that “1” means a point is in the set of k nearest neighbours of another point; and “0” otherwise. Thus, a k -means clustering algorithm can be used to group points based on their k NN graph.

However, k NN kernel cannot be applied to both density-based clustering and k NN anomaly detection. This is because it converts all points to have the same density in the new space regardless of the bandwidth used by a density estimator used by the intended algorithm. Thus, DBSCAN will either group neighbouring clusters into a single cluster or assign all clusters to noise. This outcome is not conducive in producing a good clustering result.

DP also cannot work with k NN kernel for the same reason. DP links a point to another point with a higher density to form clusters in the last step of the clustering process²⁹. DP would not be able to link points when all points have the same density.

For k NN anomaly detection, replacing the distance measure with the k NN kernel produces either 0 or 1 similarity between any two points. This does not work for anomaly detection.

8 Conclusions

We introduce a CDF Transform-Shift (CDF-TS) algorithm based on a multi-dimensional CDF transform to effectively deal with datasets with inhomogeneous densities. It is the first attempt to change the volumes of every point’s neighbourhood in the entire multi-dimensional space in order to get the desired effect of uniform distribution for the whole dataset w.r.t a density estimator. Existing CDF transform methods such as ReScale³⁶ and DScale³⁷ achieved a much reduced effect on the rescaled dataset. We show that this more sophisticated CDF transform brings about a much better outcome.

In addition, CDF-TS is more generic than existing CDF transform methods with the ability to use different density estimators, i.e, uniform kernels with either fixed or variable bandwidths. As a result, CDF-TS can be applied to more algorithms/tasks with a better outcome than existing methods such as k NN kernel²⁶.

Through intensive evaluations, we show that CDF-TS significantly improves the performance of two existing density-based clustering algorithms and one existing distance-based anomaly detector.

Appendix: DScale algorithm

Algorithm 2 is a generalisation of the implementation of DScale³⁷ which can employ a density estimator with a bandwidth parameter λ . It requires one parameter λ only.

Algorithm 2 DScale(S, λ, d)

Input: S - input distance matrix ($n \times n$ matrix); λ - bandwidth parameter; d - dimensionality of the dataset.**Output:** S' - distance matrix after scaling.

```

1:  $m \leftarrow$  the maximum distance in  $S$ 
2: Initialising  $n \times n$  matrix  $S'$ 
3: for  $i = 1$  to  $n$  do
4:    $r(x_i) = \frac{m}{\lambda} \times \left( \frac{|\mathcal{N}(x_i, s, \lambda)|}{n} \right)^{\frac{1}{d}}$ 
5:    $\forall_{x_j \in \mathcal{N}(x_i, s, \lambda)} S'[x_i, x_j] = S[x_i, x_j] \times r(x_i)$ 
6:    $\forall_{x_j \in D \setminus \mathcal{N}(x_i, s, \lambda)} S'[x_i, x_j] = (S[x_i, x_j] - \lambda) \times \frac{m - \lambda \times r(x_i)}{m - \lambda} + \lambda \times r(x_i)$ 
7: end for
8: return  $S'$ 

```

References

1. Charu C Aggarwal. *Outlier Analysis*. Springer International Publishing, Switzerland, 2nd edition, 2017. ISBN 978-3-319-47577-6.
2. Charu C Aggarwal and Chandan K Reddy. *Data Clustering: Algorithms and Applications*. Chapman and Hall/CRC Press, 2013.
3. Selim Aksoy and Robert M Haralick. Feature normalization and likelihood-based similarity measures for image retrieval. *Pattern recognition letters*, 22(5):563–582, 2001.
4. Fabrizio Angiulli and Clara Pizzuti. Fast outlier detection in high dimensional spaces. In *European Conference on Principles of Data Mining and Knowledge Discovery*, pages 15–27. Springer, 2002.
5. Mihael Ankerst, Markus M. Breunig, Hans-Peter Kriegel, and Jörg Sander. OPTICS: Ordering points to identify the clustering structure. In *Proceedings of the 1999 ACM SIGMOD International Conference on Management of Data*, SIGMOD ’99, pages 49–60, New York, NY, USA, 1999. ACM. ISBN 1-58113-084-8.
6. Ingwer Borg, Patrick JF Groenen, and Patrick Mair. *Applied Multidimensional Scaling*. Springer Science & Business Media, 2012.
7. Markus M. Breunig, Hans-Peter Kriegel, Raymond T. Ng, and Jörg Sander. LOF: Identifying density-based local outliers. *SIGMOD Rec.*, 29(2):93–104, May 2000.
8. Varun Chandola, Arindam Banerjee, and Vipin Kumar. Anomaly detection: A survey. *ACM computing surveys (CSUR)*, 41(3):15, 2009.
9. Timothy De Vries, Sanjay Chawla, and Michael E Houle. Finding local anomalies in very high dimensional space. In *Data Mining (ICDM), 2010 IEEE 10th International Conference on*, pages 128–137. IEEE, 2010.
10. Janez Demšar. Statistical comparisons of classifiers over multiple data sets. *Journal of Machine Learning Research*, 7:1–30, 2006.
11. Dua Dheeru and Efi Karra Taniskidou. UCI machine learning repository, 2017. URL <http://archive.ics.uci.edu/ml>.
12. Levent Ertöz, Michael Steinbach, and Vipin Kumar. Finding topics in collections of documents: A shared nearest neighbor approach. *Clustering and Information Retrieval*, 11:83–103, 2003.
13. Levent Ertöz, Michael Steinbach, and Vipin Kumar. Finding clusters of different sizes, shapes, and densities in noisy, high dimensional data. In *Proceedings of the 2003 SIAM International Conference on Data Mining*, pages 47–58. SIAM, 2003.
14. Martin Ester, Hans-Peter Kriegel, Jörg S, and Xiaowei Xu. A density-based algorithm for discovering clusters in large spatial databases with noise. In *Proceedings of the Second International Conference on Knowledge Discovery and Data Mining (KDD-96)*, pages 226–231. AAAI Press, 1996.
15. Tom Fawcett. An introduction to roc analysis. *Pattern recognition letters*, 27(8):861–874, 2006.
16. Evelyn Fix and Joseph L Hodges Jr. Discriminatory analysis-nonparametric discrimination: consistency properties. Technical report, California Univ Berkeley, 1951.

17. Xiaofei He and Partha Niyogi. Locality preserving projections. In S. Thrun, L. K. Saul, and B. Schölkopf, editors, *Advances in Neural Information Processing Systems 16*, pages 153–160. MIT Press, 2004.
18. Ian Jolliffe. Principal component analysis. In *International encyclopedia of statistical science*, pages 1094–1096. Springer, 2011.
19. Fei Tony Liu, Kai Ming Ting, and Zhi-Hua Zhou. Isolation forest. In *2008 Eighth IEEE International Conference on Data Mining*, pages 413–422. IEEE, 2008.
20. Fei Tony Liu, Kai Ming Ting, and Zhi-Hua Zhou. On detecting clustered anomalies using SCiForest. In *Proceedings of the 2010 European Conference on Machine Learning and Knowledge Discovery in Databases: Part II*, ECML PKDD’10, pages 274–290, Berlin, Heidelberg, 2010. Springer-Verlag. ISBN 3-642-15882-X, 978-3-642-15882-7.
21. Fei Tony Liu, Kai Ming Ting, and Zhi-Hua Zhou. On detecting clustered anomalies using sciforest. In José Luis Balcázar, Francesco Bonchi, Aristides Gionis, and Michèle Sebag, editors, *Machine Learning and Knowledge Discovery in Databases*, pages 274–290, Berlin, Heidelberg, 2010. Springer Berlin Heidelberg. ISBN 978-3-642-15883-4.
22. Fei Tony Liu, Kai Ming Ting, and Zhi-Hua Zhou. Isolation-based anomaly detection. *ACM Transactions on Knowledge Discovery from Data (TKDD)*, 6(1):3:1–3:39, March 2012. ISSN 1556-4681.
23. Don O Loftsgaarden, Charles P Quesenberry, et al. A nonparametric estimate of a multivariate density function. *The Annals of Mathematical Statistics*, 36(3):1049–1051, 1965.
24. Laurens van der Maaten and Geoffrey Hinton. Visualizing data using t-sne. *Journal of machine learning research*, 9(Nov):2579–2605, 2008.
25. James MacQueen. Some methods for classification and analysis of multivariate observations. In *Proceedings of the fifth Berkeley symposium on mathematical statistics and probability*, volume 1, pages 281–297. Oakland, CA, USA, 1967.
26. D. Marin, M. Tang, I. Ben Ayed, and Y. Y. Boykov. Kernel clustering: density biases and solutions. *IEEE Transactions on Pattern Analysis and Machine Intelligence*, pages 1–1, 2018. ISSN 0162-8828. doi: 10.1109/TPAMI.2017.2780166.
27. Sridhar Ramaswamy, Rajeev Rastogi, and Kyuseok Shim. Efficient algorithms for mining outliers from large data sets. In *Proceedings of the 2000 ACM SIGMOD International Conference on Management of Data*, SIGMOD ’00, pages 427–438, New York, NY, USA, 2000. ACM. ISBN 1-58113-217-4.
28. C. J. Van Rijsbergen. *Information Retrieval*. Butterworth-Heinemann, Newton, MA, USA, 2nd edition, 1979. ISBN 0408709294.
29. Alex Rodriguez and Alessandro Laio. Clustering by fast search and find of density peaks. *Science*, 344(6191):1492–1496, 2014.
30. Bernhard Schölkopf, Alexander J Smola, et al. *Learning with kernels: support vector machines, regularization, optimization, and beyond*. MIT press, Cambridge, 2002.
31. Alexander Strehl and Joydeep Ghosh. Cluster ensembles—a knowledge reuse framework for combining multiple partitions. *Journal of Machine Learning Research*, 3(Dec):583–617, 2002.
32. Richard Szeliski. *Computer vision: algorithms and applications*. Springer Science & Business Media, 2010.
33. Joshua B Tenenbaum, Vin De Silva, and John C Langford. A global geometric framework for nonlinear dimensionality reduction. *science*, 290(5500):2319–2323, 2000.
34. Fei Wang and Jimeng Sun. Survey on distance metric learning and dimensionality reduction in data mining. *Data Mining and Knowledge Discovery*, 29(2), 2015.
35. Fei Wang, Bin Zhao, and Changshui Zhang. Unsupervised large margin discriminative projection. *IEEE transactions on neural networks*, 22(9):1446–1456, 2011.
36. Ye Zhu, Kai Ming Ting, and Mark J. Carman. Density-ratio based clustering for discovering clusters with varying densities. *Pattern Recognition*, 60:983 – 997, 2016. ISSN 0031-3203.

37. Ye Zhu, Kai Ming Ting, and Maia Angelova. A distance scaling method to improve density-based clustering. In Dinh Phung, Vincent S. Tseng, Geoffrey I. Webb, Bao Ho, Mohadeseh Ganji, and Lida Rashidi, editors, *Advances in Knowledge Discovery and Data Mining*, pages 389–400, Cham, 2018. Springer International Publishing. ISBN 978-3-319-93040-4.